Studies of the Relationship between Bilayer Water Permeability and Bilayer Physical State†

A. Carruthers* and D. L. Melchior*

ABSTRACT: The relationship between osmotic water permeability and bilayer physical state was examined in large unilamellar vesicles (LUVs) by using microturbidimetry and differential scanning calorimetry. Permeability was found to largely reflect the physical state of the lipid bilayer. A transition from low to high permeability parallels the bilayer liquid-crystalline to fluid phase transition. In the fluid state, the permeabilities of most lecithin bilayers are similar, being more than 2 orders of magnitude greater than when crystalline. At temperatures well below or well above the phase transition onset temperature, the permeabilities of fully fluid and fully crystalline lecithin bilayers show little dependence on temperature. Cholesterol, at 5 mol %, increases the permeability of dimyristoylphosphatidylcholine (DML) LUVs at temperatures below the completion of the phase transition. At higher temperatures, 5 mol % cholesterol reduces DML bilayer permeability. At all temperatures, increasing cholesterol from 10 to 27 mol % produces a monotonic decrease in DML bilayer permeability. Thereafter, increasing bilayer cholesterol serves to increase permeability. The permeability of bilayers formed from two lipids showing phase separation also parallels the physical state of the membranes. LUVs formed from total lipids extracted from human erythrocytes show quantitatively similar permeability properties to LUVs formed from synthetic lipids. Reconstitution of human erythrocyte integral membrane proteins into lecithin bilayers increases both water and D-glucose permeability by some 30–100-fold. This increased water permeability is independent of the bilayer physical state and is similar, kinetically, to human erythrocyte water permeability. We conclude that native membrane water permeability derives from the interaction of protein with the lipid bilayer. In the absence of protein, permeability is governed by bilayer physical state.

Unilamellar vesicles formed from synthetic or native lipids exhibit permeability characteristics resembling those of biological membranes. The effects of steroids, ionophores, polyenes, anaesthetics, and lytic agents on the transbilayer flux of encapsulated solute in these model membrane systems are similar to those observed in biological membranes (Weissman et al., 1966; De Gier et al., 1970; Bangham et al., 1965). As the diffusion of small molecules across synthetic bilayers is influenced by the degree of packing and thermal mobility of the lipid hydrocarbon chains (Van Deenen, 1971), these studies have led to the view that the physical state of the native bilayer may play some role in the regulation of membrane permeability.

We have examined this possibility by using the turbidimetric method (Tedeschi & Harris, 1955, 1958; Sidal & Solomon, 1957; Sha'afi et al., 1967; Kamino & Inouye, 1969; Bangham et al., 1967; Bittman & Blau, 1972) for the determination of osmotically induced transbilayer water flux rates. We have investigated the effects of altered bilayer physical state on water permeability and the influence of cholesterol on this phenomenon. Further, we have determined water permeability coefficients in vesicles formed from lipid mixtures, in vesicles formed from extracted native lipids, and in vesicles containing reconstituted bilayer-spanning proteins. We conclude that vesicle water permeability does indeed reflect the physical state of the bilayer, albeit in a complex fashion. Furthermore, the greatest determinant of native bilayer water permeability seems not to be bilayer physical state but the presence of bilayer-spanning proteins in the membrane.

Materials and Methods

Solutions. Isotonic medium consisted of 100 mM D-glucose, 10 mM KCl, and 0.2 mM (Hepes),[1] pH 7.2. Hypotonic medium consisted of 10 mM KCl and 0.2 mM Hepes, pH 7.2. All other solutions were as described in the text and, in addition, were buffered to pH 7.2 with 0.2 mM Hepes.

Vesicles. Large unilamellar vesicles (LUVs) were formed from synthetic or native lipids either by dialysis (see protein reconstitution) or by reverse-phase evaporation (Szoka & Papahadjopoulos, 1980). With the latter procedure, lipids supplied in hexane or lipid mixtures formed in chloroform were first dried down to a thin film on the bottom of a round-bottomed flask (50 mL) under a stream of N_2. Any remaining organic solvent was then removed in vacuo (100 μmHg) for 3–48 h. The lipid film (50 mg) was resuspended in 1.5 mL of diethyl ether, and then 0.5 mL of isotonic medium was added. This mixture was sonicated for 2–5 min in a bath-type sonicator, and then the organic solvent was removed by rotary evaporation under reduced pressure. This step was always carried out at a temperature greater than the T_m of the highest melting point lipid in the flask. The resulting gel was dispersed in isotonic medium, and the resulting LUVs were collected by centrifugation at 45000*g* for 20 min.

The mean isotonic diameter of LUVs formed in this way was determined both by electron microscopy using a negative stain and by use of the Coulter-N4 multichannel Submicron Particle Sizer (Coulter Electronics, Hialeah, FL). The obtained diameters were 0.36 ± 0.03 and 0.34 ± 0.05 μm, respectively. Pelleted LUV volumes were determined by centrifugation of LUV suspensions in calibrated glass capillaries. Extravesicular pellet volumes were determined by adding

† From the Department of Biochemistry, University of Massachusetts Medical School, Worcester, Massachusetts 01605. *Received June 7, 1983.*

[1] Abbreviations: LUVs, large unilamellar vesicles; DSC, differential scanning calorimetry; DML, dimyristoyllecithin; DPL, dipalmitoyllecithin; DOL, dioleoyllecithin; DSL, distearoyllecithin; DEL, dielaidoyllecithin; egg PC, egg phosphatidylcholine; PE, phosphatidylethanolamine; Chol, cholesterol; Hepes, *N*-(2-hydroxyethyl)piperazine-*N*'-2-ethanesulfonic acid; EGTA, ethylene glycol bis(β-aminoethyl ether)-*N*,*N*,*N*',*N*'-tetraacetic acid; EDTA, ethylenediaminetetraacetic acid; FID, free induction decay; GC, gas chromatograph; Tris, tris(hydroxymethyl)aminomethane; CCB, cytochalasin B.

0006-2960/83/0422-5797$01.50/0

[^{3}H]inulin to the extravesicular medium and measuring the wet and dry weights of pelleted LUVs. Extravesicular volumes vary from 55 to 91% of total pellet volumes. This variation arises from different centrifugation speeds. Isotonic encapsulated volumes range from 1.2 to 3.7 μL/μmol of lipid.

Protein Reconstitution. Human erythrocyte ghosts were prepared as described by Carruthers & Melchior (1983). Peripheral proteins were eluted by successive EDTA and salt washes of the ghosts (Kasahara & Hinkle, 1977). The remaining integral proteins (bands 3, 4.5, and 7) were solubilized by using 0.5% Triton X-100. After centrifugation of the solubilized membranes (100000*g*, 1 h), the supernatant was treated with Biobeads (SM2) overnight to remove Triton X-100 (Kasahara & Hinkle, 1977). The resulting protein/lipid suspension was added to a mixed micellar solution of lipid to give final concentrations of 35 mM lipid, 35 mM cholate, 5 mg of protein/100 mg of lipid, 40 mM Hepes, and 20 mM D-glucose, pH 8.6. Cholate was then removed by defined dialysis at 20 ± 1 °C against cholate-free medium for 24 h. The ratio of dialysis medium to dialysate was constant at 1000:1, and the dialysis medium was replaced with fresh medium at a rate of 0.2% min^{-1}. The resulting vesicles were concentrated either by vacuum dialysis or by centrifugation at 45000*g* for 30 min. The average diameter of egg lecithin vesicles (with or without protein) formed in this way was 0.36 ± 0.03 μm (n = 50). Proteins were also reconstituted by reverse-phase evaporation. Here, the cholate-free protein solution was added to the etheric lipid solution prior to sonication. Cytochalasin B inhibitable D-glucose fluxes (Figure 10) indicated that functional reconstitution of the D-glucose transport proteins had been achieved by using both techniques.

Physical State of Membranes. The physical state of native and LUV membranes was characterized by differential scanning calorimetry (Melchior et al., 1977) using the computerized Du Pont 1090 Thermal Analysis System. Thermograms were analyzed (transition onset and completion temperatures, enthalpies, partial areas, weighted normalizations, etc.) by using the Du Pont General Analysis and File Modification data analysis programs.

Pelleted red cell ghosts and LUVs (15 μL) were loaded into calorimeter pans, and, where appropriate, the lipid content was determined by parallel dry weight estimates. The average mass of lipid per pan was 1 mg. The obtained thermograms were independent of the scan rate.

Osmotic Water Permeability. Changes in vesicular volume induced by osmotic water flow were monitored in a continuous fashion by spectrophotometry [turbidimetry, see Tedeschi & Harris (1955, 1958), Sidel & Solomon (1957), Rendi (1964), Bangham et al. (1967), Kamino & Inouye (1969), Reeves & Dowben (1970), and Bittman & Blau (1972)]. The microturbidimetric analysis system was that described by Carruthers & Melchior (1983) for use in hexose transfer determinations with the following modifications. (1) Temperature control and vesicle injection into the light path of the spectrophotometer were controlled by computer. (2) On-line data acquisition and analysis were performed by computer. (3) The data storage medium was magnetic (floppy discs). Analog inputs to an Apple II Plus computer were converted to digital inputs with 12-bit resolution over a 0–100-mV, or a −100- to +100-mV input range (conversion time, 20 μs; AI13, Interactive Structures, Inc.). Parallel digital command signals were generated by using a Digital Interface (DI09, Interactive Structures, Inc.). Data acquisition and command signals were controlled by short machine language routines called from larger programs written in BASIC. With this method, analog data could be sampled at rates up to 20 kHz.

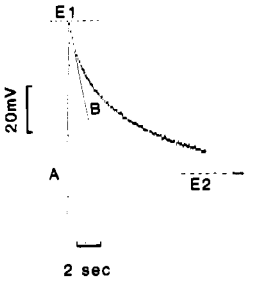

FIGURE 1: Measurement of initial rate of vesicular swelling. The spectrophotometer output (absorbance at 500 nm) was digitized and stored as a two-dimensional array with respect to time. Slope A represents the initial mixing of 0.5 μL of packed DML LUVs and 400 μL of hypotonic medium and equilibration of the spectrophotometer output. Slope B represents the initial rate of swelling of the vesicles. The intersection of slopes A and B (E_1) is equivalent to the steady-state absorbance of LUVs prior to swelling. E_2 is the absorbance level at osmotic equilibrium. The linear sections of slopes A and B were selected by the user; then the slope of the points within these ranges was calculated by the method of least squares. The rate of swelling, dV/dt (percent per second), was expressed as $100[B/(E_1 - E_2)]$ where $B = dE$ per second. Temperature, 27.5 °C.

Procedures. Packed LUVs containing isotonic medium (total volume 0.5 μL) were injected into 400 μL of hypotonic medium. Mixing and transport of the LUV suspension to the light path of the spectrophotometer were effected within 100 ms. The turbidity of this suspension was monitored at 500 nm at sample rates between 10 and 0.5 Hz. Turbidity decreases with increasing intravesicular volume. As the refractive index of the medium is constant, the change in turbidity on injection of LUVs into medium depends only on the relative volume change and the initial difference between the refractive index of the medium and intravesicular solution [see Reeves & Dowben (1970)]. Figure 1 shows a typical record obtained on injection of LUVs into hypotonic medium. Slope A represents the rapid upward movement of the recording device (monitor gun) and slope B the initial rate of vesicle swelling (change in turbidity). The initial apparent absorbance level (volume), E_1, is given by the intersection of slopes A and B. The initial percentile rate of turbidity/volume change is, therefore, given by $100[B/(E_1 - E_2)]$ per second where B is dE per second. The linear segments of slopes A and B were user determined; the remaining regression analyses were software controlled. Swelling records obtained at different wavelengths (331–726 nm) were essentially identical with those obtained at 500 nm. $B/(E_1 - E_2)$ was independent of wavelength. The electronic signal to noise ratio at steady-state turbidity levels was on the order of 1000:1.

It has been shown that the D-glucose permeability of synthetic membranes at temperatures in the vicinity of the onset of the bilayer melt (T_m) is sensitive to temperature shock (Blok et al., 1976). If glucose-loaded vesicles are preequilibrated to the temperature of the medium into which they are to be injected, the rate of loss of vesicular sugar following injection is much lower than that observed without temperature preequilibration. Our stop-flow system is designed such that vesicles and hypotonic medium are temperature controlled to within 0.1 °C of each other prior to mixing (Carruthers & Melchior, 1983). This avoids temperature change, lipid phase perturbation, and subsequent significant loss of vesicular glucose on mixing of LUVs and hypotonic medium. This is important, for the rate of transbilayer water flux is determined by the transmembrane glucose concentration/osmotic gradient.

Modification of the Cholesterol Content of Red Cell Membranes. Red cell ghosts [prepared as described by

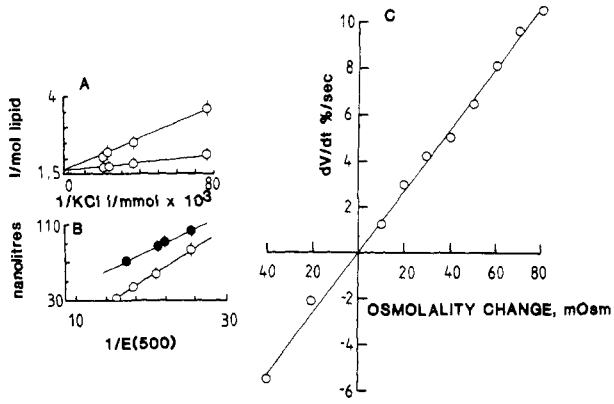

FIGURE 2: (A) Osmotic swelling of DML LUVs formed in 100 mM KCl and injected into diluted KCl medium. The equilibrium-encapsulated volumes (liters per mole of lipid) are plotted vs. the reciprocal of the extravesicular KCl concentration. Each point represents the mean (±SE) of three or more separate determinations at 10 °C. Extrapolation to infinite salt concentration gives the volume of the osmotic dead space. (B) Vesicle-encapsulated volume (nanoliters per 0.02 μmol of lipid) plotted against the reciprocal of the steady-state absorption at 500 nm for dispersion at a concentration of 0.05 μmol/mL. Vesicle composition: (●) cholesterol/DML (1:1 molar ratio), 20 °C; (○) DML, 10 °C. The LUVs were formed in 75 mM KCl medium, and 0.5 μL of packed LUVs was injected into various KCl concentrations. Each point represents the mean ± SE of at least four determinations. (C) Effect of the initial transmembrane osmotic gradient on the initial rate of volume change: ordinate, rate of volume change; abscissa, initial transmembrane osmotic difference (milliosmolar). The LUVs [DOL/egg yolk sphingomyelin/cholesterol (1:1:0.5)] were formed in 100 mM D-glucose and 10 mM KCl and injected into 10 mM KCl containing an appropriate D-glucose concentration. Negative values of dV/dt represent shrinkage and positive values swelling. Each point represents the mean of two determinations at 20.0 °C.

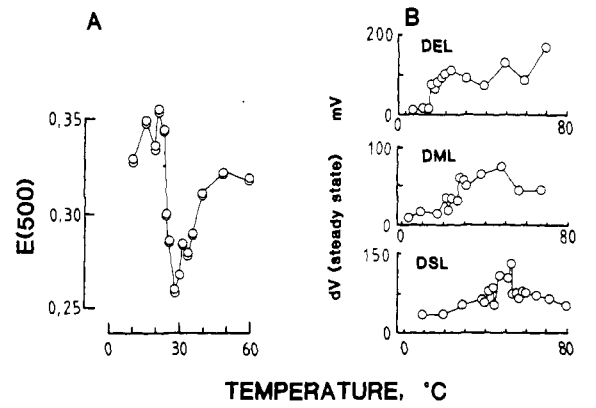

FIGURE 3: (A) Steady-state isotonic apparent absorbance of DML LUVs vs. temperature. 0.5 μL of packed LUVs was injected into 0.4 mL of isotonic medium. Both LUVs and medium were preequilibrated to the desired temperature prior to mixing. (B) Change in absorbance of various LUV types (DEL, DML, and DSL) on injection into hypotonic medium vs. temperature of the medium. 0.5 μL of LUVs was injected into 400 μL of hypotonic medium. Steady-state absorbance changes ($E_1 - E_2$, see Figure 1) are expressed as millivolts. Each point represents the mean of at least three separate determinations.

Carruthers & Melchior (1983)] were partially depleted of their cholesterol content by exposure to sonicated egg lecithin dispersions [see Masaik & LeFevre (1974)]. Cholesterol and phospholipid phosphorus assays were as described by Gamble et al. (1979) and Bartlett (1959), respectively.

Materials and Lipid and Protein Analysis. All lipids (other than red cell lipids) and chemicals were purchased from Sigma (St. Louis, MO). Red cell lipids were extracted under N_2 by a modified method of Bligh & Dyer (1959). All lipids were stored at −22 °C under N_2. The class composition of the red cell lipids was quantitated by using an Iatroscan TH-10 FID (Ackman, 1981). The class purity of the synthetic lipids was confirmed with the Iatroscan FID and their fatty acid composition by a Varian 3700 GC (Palo Alto, CA) with a 30-m SP 2330 capillary (Supelco, Bellfonte, PA). Protein assays were performed according to the method of Lowry et al. (1951).

Results

General Observations. Water permeability determinations using the light-scattering method require that LUVs behave as perfect osmometers and that the relationship between apparent absorbance and vesicle volume is linear. Figure 2 shows that both requirements are satisfied.

The encapsulated volumes of swollen large unilamellar vesicles increase in accordance with the Boyle–van't Hoff law; i.e., $V = K/C + V_{c\to\infty}$ where V is volume, C the salt concentration, K a constant, and $V_{c\to\infty}$ the osmotic dead space. Similar findings have been described for multilamellar vesicles (Bangham et al., 1967; Blok et al., 1976). In Figure 2A, two separate experiments with dimyristoyllecithin (DML) LUVs are shown, and while they differ in slope (K), they indicate the same osmotic dead space.

The relationship between the encapsulated vesicle volume and the turbidity of the corresponding vesicle dispersions is shown in Figure 2B. Here, the encapsulated vesicle volumes of DML LUVs and DML/cholesterol (1:1) LUVs as formed, swollen or contracted, are plotted against the reciprocal of apparent absorbance. The linear relationship confirms the validity of optical measurements. Earlier experiments (Bangham et al., 1967; Blok et al., 1976) also confirm this for multilamellar vesicles.

Figure 2C shows the relationship between the initial rate of change of $1/E$ (expressed as a percentage of the total absorbance change) and the initial transbilayer osmotic difference in DML/egg yolk sphingomyelin/cholesterol (1:1:0.5) LUVs. The linear relationship is in close agreement with earlier observations (Bangham et al., 1967; Bittman & Blau, 1972). These observations establish the validity and accuracy of the turbidimetric method for determination of changes in vesicle volume. Moreover, this procedure permits real-time analysis and precision temperature control. These features are not possible with isotopic flux determinations.

Effects of Temperature on Steady-State Absorbance Measurements. The relationship between temperature and the isotonic steady-state apparent absorbance of DML LUVs (0.25 mg of DML/mL) is shown in Figure 3A. As temperature is raised and the bilayers begin to melt (see Figure 4A), there is a marked decrease in turbidity. On completion of the bilayer phase transition, the turbidity returns close to control levels. This reversible change in the apparent absorbance corresponds to the "normal" reversible change in turbidity arising from changes in the index of refraction of the bilayer associated with the membrane phase transition (Yi & MacDonald, 1973; Chong & Colbow, 1976; Avramovic-Zikic & Colbow, 1978).

Figure 3B illustrates the relationship between temperatue and the magnitude of the turbidity change on injection of LUVs into hypotonic medium. These turbidity changes are superimposed on the steady-state turbidity measured at isotonic volume and vary between 22 and 109% of this steady-state turbidity. With distearoyllecithin (DSL), DML, and dielaidoyllecithin (DEL), there is an abrupt increase in the magnitude of the turbidity change associated with the bilayer phase transition. DSL and DML show some recovery on completion of the phase transition. These turbidity changes

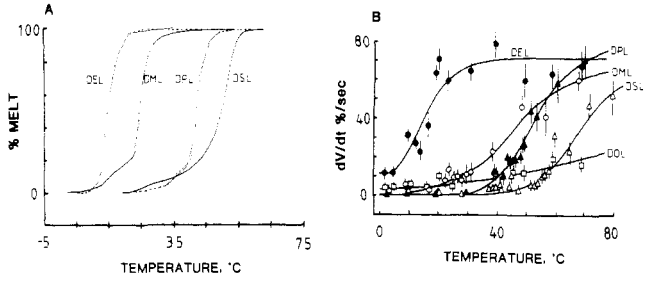

FIGURE 4: (A) Physical state of various lecithin LUV bilayers (DEL, DML, DPL, and DSL). The ordinate represents the percentage melt of the membranes. 100% melt indicates fully fluid bilayer, and 0% melt indicates crystalline bilayer. These curves were calculated from the DSC thermograms of the LUVs used in (B). The foot on each curve represents the pretransition melt. (B) Osmotic water permeability of DOL (□), DEL (●), DML (○), DPL (▲), and DSL (△) LUVs as a function of temperature. Conditions as described in Figure 3B. Each point represents the mean ± SE of at least three determinations. The curves through the points were drawn by eye.

do not seem to reflect altered intravesicular volume changes with increasing temperature. Analysis of pellet volume changes on injection of temperature-equilibrated DML LUVs into hypotonic medium at 4, 21.2, and 36.8 °C shows only a modest volume increase occurring between 4 and 37 °C relative to changes in apparent absorbance (pellet volume increase at 4 °C, 6.5%; pellet volume increase at 36.8 °C, 6.8%; apparent absorbance change at 4 °C, 15%; apparent absorbance change at 36.8 °C, 74%; number of measurements, three or more). This is in agreement with these changes resulting from an altered refractive index of the bilayers.

Water Permeability and Physical State of Pure Bilayers. The relationship between bilayer physical state and the initial rate of osmotically induced volume change (swelling) in LUVs formed from a variety of lipid species is shown in Figure 4. The LUVs were formed from either dioleoyllecithin (DOL), DML, dipalmitoyllecithin (DPL), DEL, or DSL. In all cases (except DOL where the bilayers melt below 0 °C), an abrupt increase in the rate of volume change is observed as the bilayers begin to melt. With lipid bilayers melting at low temperatures (DOL and DEL), the rate of osmotically induced volume change appears to increase less rapidly with increasing temperature above the melt than with DPL, DSL, or DML. This observation, however, may be a consequence of a less extensive temperature range studied above the melting temperature of the higher melting point lipids. The most notable difference between the bilayer types is the very low permeability of fluid DOL and egg lecithin bilayers. The possible influence of residual ether in the bilayers formed by reverse-phase evaporation is unlikely. Addition of 0.1% diethyl ether to DML LUVs increases the rate of osmotically induced swelling some 5-fold at all temperatures, yet the behavior of control LUVs is indistinguishable from that of multilamellar DML vesicles formed in the absence of organic solvent.

It is possible to calculate the osmotic water permeability coefficient, P_f, of these vesicle types if we know the magnitude of the volume change and the relationship between vesicle size and apparent absorbance. P_f is related to rate of change of vesicle volume in the following way:

$$P_f = \frac{dV}{dt}\frac{1}{A\pi}\left[\frac{55.6(22.4T)}{273}\right] \quad (1)$$

where V = volume, A = surface area, t = time, T = temperature (kelvin), and π is the transbilayer osmotic gradient in atmospheres which is given by $RT[(g_1m_1 + g_2m_2) - (g_1'm_1' + g_2'm_2')]$. g and m refer to the osmotic coefficients and molalities of species 1 and 2, respectively, at cis (e.g., g_1) or trans (g_1') sides of the bilayer. The term in brackets in eq 1 converts to an infinite salt gradient.

Table I: Osmotic Water Permeability (P_f) of Protein-Free Bilayers

lipid	P_f (cm·s^{-1})[a] 10 °C below transition	n[b]	10 °C above transition	n
DML	$(1.99 \pm 0.08) \times 10^{-5}$	4	$(5.98 \pm 0.21) \times 10^{-4}$	4
DPL	$(4.74 \pm 0.32) \times 10^{-6}$	5	$(6.32 \pm 0.18) \times 10^{-4}$	5
DOL	NA[c]		$(2.3 \pm 0.2) \times 10^{-4}$[e]	5
DSL	$(9.32 \pm 0.21) \times 10^{-6}$	4	$(2.8 \pm 0.3) \times 10^{-4}$	3
DEL	$(0.91 \pm 0.06) \times 10^{-4}$	4	$(7.51 \pm 0.29) \times 10^{-4}$	3
egg PC	NA		$(2.05 \pm 0.13) \times 10^{-4}$[e]	4
DML/Chol[d] (1:1)	NA		$(2.14 \pm 0.18) \times 10^{-4}$	3
DPL/Chol[d] (1:1)	NA		$(7.16 \pm 0.32) \times 10^{-5}$	4

[a] Values are given as the mean ± the standard error of the mean. [b] n is the number of determinations. [c] NA implies that no transition could be determined above 0 °C. Therefore, measurements below the transition were not possible. [d] With cholesterol additions, P was measured at the same temperatures as in cholesterol-free fluid DML and DPL vesicles. [e] Permeability measured at 20 °C.

In principle, it is necessary to determine the absolute magnitude of volume changes and area changes and the relationship between volume and apparent absorbance for each vesicle type at each temperature studied. In practice, we have found that, as expected, the magnitude of the osmotically induced volume change does not seem to be affected markedly by temperature or vesicle type. Furthermore, the relationship between turbidity and the reciprocal of vesicle size is linear. Knowing this, we can determine approximate values for P_f in the various LUVs studied. Table I summarizes our calculations for LUVs at temperatures where the bilayers are either crystalline or fluid. Here, we have assumed that surface area changes are negligible; i.e., during swelling, the vesicles undergo a transition from a flattened to a more spherical shape. This seems reasonable, for the 2.4-fold increase in volume observed with DML/cholesterol LUVs (Figure 2) would require an increase in surface area of 1.8-fold if swollen and isotonic vesicles are spherical. Earlier studies have noted the nonspherical appearance of liposomes at isotonic volume (Bangham et al., 1967).

Effects of Cholesterol on Membrane Permeability and Physical State. Since cholesterol greatly reduces transbilayer Na^+ flux (Papahadjopoulos et al., 1973), we examined its effect on both water permeability and the thermal behavior of dimyristoyllecithin LUVs. Figures 5–7 summarize our findings. Figures 5 and 7A show the effect of cholesterol on the thermal properties of DML LUVs. As the molar ratio of cholesterol in the bilayer increases from 0 to 0.05, the pretransition of DML is abolished, and the heat of the melt decreases. From 15 to 34% cholesterol, the transition broadens and now consists of two components—a narrow, well-defined component which decreases with increasing cholesterol and is presumably pure DML, and a broader component which may be some DML/cholesterol complex.

At 40–50% cholesterol, the broader transition is barely discernible, yet a melt centering about 22 °C is still present, albeit greatly diminished, and represents, presumably, traces of pure DML undergoing a crystalline to fluid transition.

The water permeability of DML/cholesterol mixtures is illustrated in Figures 6 and 7B. The behavior of these membranes is rather more complex than that of pure lipid bilayers.

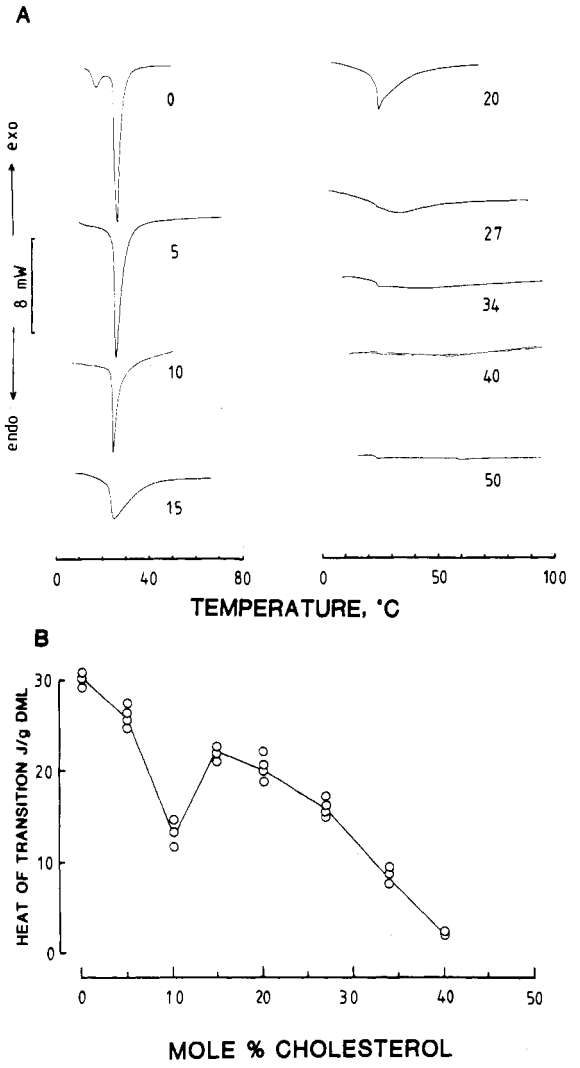

FIGURE 5: Effects of cholesterol on the physical state of DML LUVs. (A) DSC thermograms (normalized with the Du Pont File Modification Program, to 1.42 mg of DML) of DML LUV bilayers containing 0, 5, 10, 15, 20, 27, 34, 40, and 50 mol % cholesterol. Scan rate, 10 °C/min. (B) Heat of transition of bilayers shown in (A) vs. mole percent cholesterol. The heat of the transition is expressed as joules per gram of DML.

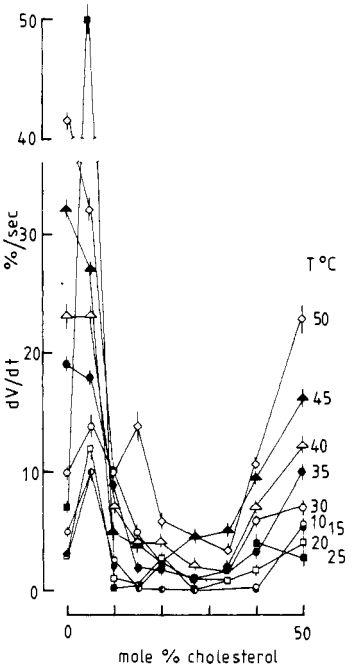

FIGURE 6: Osmotic water permeability of DML LUVs vs. mole percent cholesterol content of the bilayers at different temperatures. Conditions as in Figure 3B. The temperature (degrees centigrade) is shown to the right of the points. Each point represents the mean ± SE of at least three separate determinations. These LUVs are those shown in Figure 5.

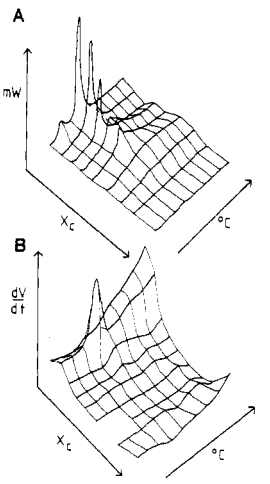

FIGURE 7: (A) Three-dimensional (X_c–mW–T) surface of the physical state of DML LUV bilayers. The x axis is the mole percent cholesterol (X_c) from 0 to 50 mol %. The y axis is the heat flow [milliwatts (mW)] from 0.13 to 1.4 mW. The z axis is the temperature (T, degrees centigrade) from 10 to 50 °C. The data are obtained from Figure 5A. (B) Three-dimensional [X_c–(dV/dt)–T] surface of the water permeability properties of DML LUVs. The x axis and z axis are as in (A). The y axis is the initial rate of volume change (dV/dt) from 0 to 50%/s on injection of the LUVs into hypotonic solution. The data are derived from Figure 6.

Cholesterol appears to have a biphasic effect on water fluxes. Increasing the cholesterol concentration from 0 to 10 mol % and from 10 to 27 mol % reduces the water flux greatly. However, further increases to 50 mol % cholesterol result in the monotonic increase in water permeability. An interesting exception is 5 mol % cholesterol, which increases the permeability of the bilayer to water. This effect is most apparent at 25 °C (the midpoint of the transition). At temperatures above the transition, 5% cholesterol reduces bilayer water permeability. Table I shows that water flux in DPL LUVs containing 50 mol % cholesterol is more severely attenuated than in DML/cholesterol (1:1) LUVs.

Water Permeability in Binary Systems. It has been suggested that boundary regions between liquid and solid lipid domains may serve as low-resistance (high-permeability) shunt pathways (Papahadjopoulos et al., 1973). One means of examining this possibility is to measure water permeability in LUVs formed from a mixture of two lipid species showing phase separation. We have chosen two lipid mixtures for study, DSL/DOL (1:1 molar ratio) and DOL/egg yolk sphingomyelin (1:1 ratio by weight). As can be seen from Figure 8, there is good phase separation in both mixtures although in each case the T_m of the high melter of the mixture is reduced significantly, indicating that some mixing occurs.

With the DOL/DSL mixture, the water permeability of the LUVs appears to represent the sum of flux rates through each component of the bilayer. The absolute flux rates are close to the calculated flux rates through bilayers consisting of 50% DOL and 50% DSL. There is little evidence for rapid flux through boundary regions.

The behavior of the DOL/sphingomyelin mixture is somewhat more difficult to interpret. Pure egg yolk sphingomyelin bilayers show an increase in water permeability as the bilayers melt. At temperatures below the melt of sphin-

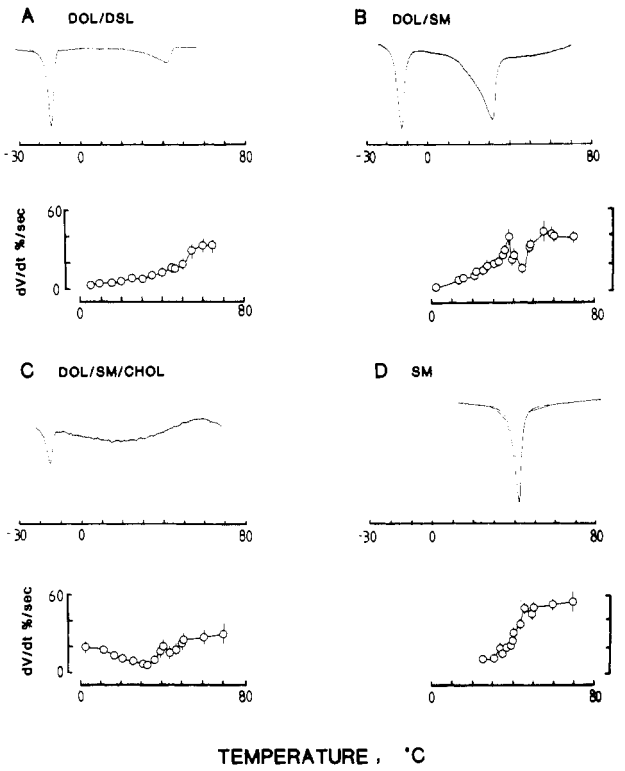

FIGURE 8: Physical state and water permeability of various LUV types vs. temperature. (A) DSC thermogram (top) and rate of volume change (bottom) in LUVs consisting of DOL and DSL (1:1 molar ratio). Conditions as in Figure 3B. DSC scan rate, 5 °C/min. (B) DSC thermogram (top) and rate of volume change (bottom) of LUVs consisting of DOL and egg yolk sphingomyelin (1:1 ratio by weight). DSC scan rate, 10 °C/min. Conditions of water flux determinations as in Figure 3B. (C) Physical state (DSC thermogram, top) and rate of volume change (bottom) in DOL/egg yolk sphingomyelin/cholesterol LUVs (1:1:0.5 molar ratio assuming sphingomyelin molecular weight = 700). DSC scan rate, 10 °C/min. (D) Physical state (DSC thermogram, top) and rate of volume change (bottom) in egg yolk sphingomyelin LUVs. DSC scan rate, 10 °C/min. With volume change measurements, each point represents the mean ± SE of at least four separate determinations. Where error bars are not seen, the error is less than the size of the point.

gomyelin bilayers, we were unable to measure water flux since the LUVs swell initially and then shrink, indicating that their contents (D-glucose) are lost to the trans solution. Bovine brain sphingomyelin displayed similar properties.

The binary system showed no such tendency to lyse at temperatures below the sphingomyelin melt, and permeability increased as the sphingomyelin became progressively more fluid. At the completion of the sphingomyelin melt, there is an abrupt decrease in permeability. Further increases in temperature serve to increase water flux. We have, therefore, some evidence for high water flux through boundary regions, but the data suggest strongly that these boundaries are between solid regions composed mostly of sphingomyelin and fluid regions containing both DOL and sphingomyelin rather than between regions of fluid DOL and solid sphingomyelin. This view is supported to some extent by the results of experiments where the sphingomyelin transition in the binary system was abolished by using 25 mol % cholesterol. Cholesterol appears to associate almost exclusively with the sphingomyelin, for the total heat of the DOL melt is reduced by less than 5%. Here, permeability seems to fall between 4 and 35 °C and thereafter increases with temperature. These results resemble those obtained with DML/cholesterol (1:1 molar ratio) LUVs (Figure 6) where permeability decreases with increasing temperature until the temperature corresponding to the completion

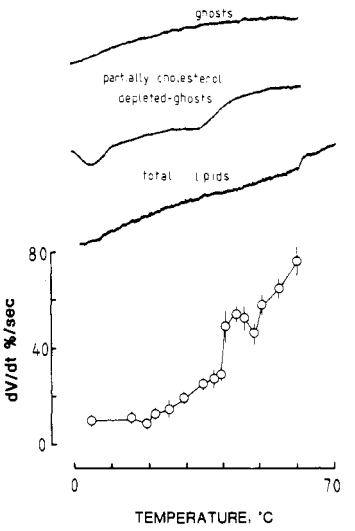

FIGURE 9: Physical state and water fluxes in LUVs formed from total red blood lipids. The top three curves are DSC scans of red cell ghosts, partially cholesterol depeleted ghosts, and LUVs formed from total red cell lipids, respectively. The ratio of cholesterol to phospholipid phosphorus in control and cholesterol-poor ghosts is 0.73 ± 0.08 and 0.25 ± 0.04, respectively. Depleted ghosts (33% hematocrit) were exposed to small unilamellar egg lecithin vesicles (180 mg/mL) for 4 h. DSC scan rate, 10 °C/min. The lower graph shows the temperature dependence of volume change in LUVs formed from total red cell lipids. Conditions as in Figure 3B. Each point represents the mean ± SE of at least three separate measurements.

of the melt of pure DML bilayers is reached.

Water Fluxes in LUVs Formed from Extracted Red Cell Lipids. It seemed of interest to determine whether the water permeability of LUVs formed from synthetic lipids resembled that of LUVs formed from lipids extracted from native membranes (human erythrocytes). Red cell lipids were extracted by the technique of Bligh & Dyer (1959) and then reconstituted into bilayers by reverse-phase evaporation. The lipid species determined by using the Iatroscan (cholesterol, 45%; phosphatidylethanolamine, 15%; phosphatidylserine, 8%; phosphatidylcholine, 15%; sphingomyelin, 17%) were in close agreement with those published elsewhere (Takemoto, 1980). Differential scanning calorimetry of these LUVs indicates a low-energy phase transition between 34 and 63 °C (Figure 9). This is absent in native red cell membranes, but appears in partially cholesterol-depleted red cell membranes (Figure 9). The presence of a transition is consistent with determinations of water permeability (Figure 9) which show a discrete break between 37 and 52 °C. We attempted to examine this further by removing cholesterol from the extracted lipids by silicic acid chromatography. Unfortunately, the cholesterol-free lipid mixture would not form vesicles by reverse-phase evaporation above or below 63 °C.

Water Fluxes in Native Bilayers and Synthetic Bilayers Containing Reconstituted Native Proteins. Human erythrocytes, human erythrocyte ghosts, and inside-out vesicles swell rapidly when mixed with hypotonic medium (Carruthers & Melchior, 1983). Inside-out vesicles and human erythrocyte ghosts were prepared and then loaded with 50 mM D-glucose in excess to the external and sealing solutions (150 mM KCl, 10 mM Tris-HCl, 50 μM cytochalasin B, and 0.2 mM EGTA, pH 7.2). The osmotic water permeability of these membranes is on the order of 0.04 cm·s^{-1} at 20 °C (vesicles, P_f = 0.043 ± 0.004 cm·s^{-1}; ghosts, P_f = 0.042 ± 0.003 cm·s^{-1}).

Water fluxes in egg lecithin LUVs containing proteins (bands 3, 4.5, and 7) reconstituted from human erythrocytes are rather slower than those observed in native membranes but are some 30-fold more rapid than those observed in pro-

Table II: Permeability (P) of Egg Lecithin Vesicles to H_2O and D-Glucose

P ($cm \cdot s^{-1}$)				
protein-free		protein-enriched		
H_2O	D-glucose	H_2O	D-glucose − CCB[a]	D-glucose + CCB[b]
1.7×10^{-4}	6.9×10^{-10}	6.3×10^{-3}	1.3×10^{-6}	1.7×10^{-9}
2.3×10^{-4}	7.4×10^{-10}	6.1×10^{-3}	1.6×10^{-6}	1.1×10^{-9}
2.2×10^{-4}	7.2×10^{-10}	5.9×10^{-3}	1.6×10^{-6}	1.3×10^{-9}
2.0×10^{-4}	7.3×10^{-10}	5.8×10^{-3}	1.5×10^{-6}	1.1×10^{-9}
$(2.05 \pm 0.13) \times 10^{-4}$[c]	$(7.2 \pm 0.1) \times 10^{-10}$[c]	$(6.03 \pm 0.11) \times 10^{-3}$[c]	$(1.5 \pm 0.07) \times 10^{-6}$[c]	$(1.3 \pm 0.14) \times 10^{-9}$[c]

[a] $P = V_{max}/K_m$; $K_m = 0.07 \pm 0.01$ mM; $V_{max} = 0.11 \pm 0.01$ pmol cm^{-2} s^{-1}. These values were obtained by integration of the time course of sugar exit (Figure 10B) according to the methods outlined by Carruthers & Melchior (1983). [b] Cytochalasin B (CCB) concentration 5 μM; temperature 20 °C. Data obtained from Figure 10 and three other sets of similar records. [c] Average values.

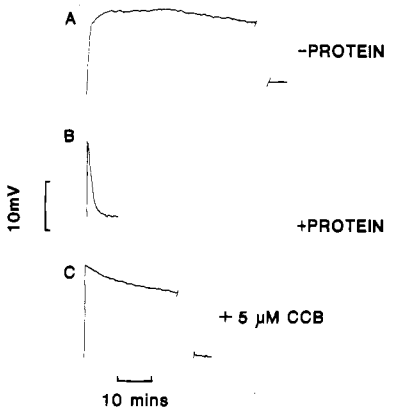

FIGURE 10: Water and sugar permeability of egg lecithin LUV membranes containing (B and C) and lacking (A) integral proteins isolated from human erythrocyte ghosts. The records are inverted for ease of interpretation. An upward deflection represents swelling and a downward deflection shrinkage. (A) Protein-free LUVs containing isotonic medium were injected into hypotonic medium at 20.0 °C. The LUVs first swell and then shrink. The final absorption level is shown to the right of the record and was achieved after 8 h. (B) Protein-rich LUVs (see Materials and Methods) containing 10 mM KCl and 30 mM D-glucose were injected into 10 mM KCl at 20.0 °C. Proteins were reconstituted by detergent dialysis. (C) As in (B) with the addition of the sugar transport inhibitor cytochalasin B (5 μM). Final equilibrium was achieved after 2 h.

tein-free egg lecithin LUVs (Figure 10). Furthermore, the sugar permeability of the protein-enriched LUVs is greater than that of protein-free LUVs. This does not arise simply from the presence of the sugar transporter (band 4.5; Jones & Nickson, 1981) in these bilayers for transporter protein function can be blocked by using cytochalasin B (see Figure 10). Table II summarizes the permeability coefficients for transbilayer water and D-glucose fluxes in protein-containing and protein-free egg lecithin LUVs. Bilayer protein appears to increase both water and sugar permeability. This effect on D-glucose permeability is both transport protein mediated and nontransport mediated. Figure 11 shows the temperature dependence of the osmotic water permeability coefficient in DPL/egg lecithin (25:75 ratio by weight) LUVs containing human erythrocyte proteins from bands 3, 4.5, and 7. This lipid mixture undergoes a broad melt between 10 and 45 °C. Water flux shows no obvious correspondence with bilayer physical state but does increase somewhat with temperature. The activation energy of this process is 3.2 kcal/mol. These proteins were reconstituted by detergent dialysis. Figure 11 also shows the water permeability properties of egg lecithin membranes containing these proteins. Here, the proteins were reconstituted by reverse-phase evaporation (absence of detergent). The striking similarity between both sets of data indicates that this enhanced water permeability does not result from residual bilayer detergent.

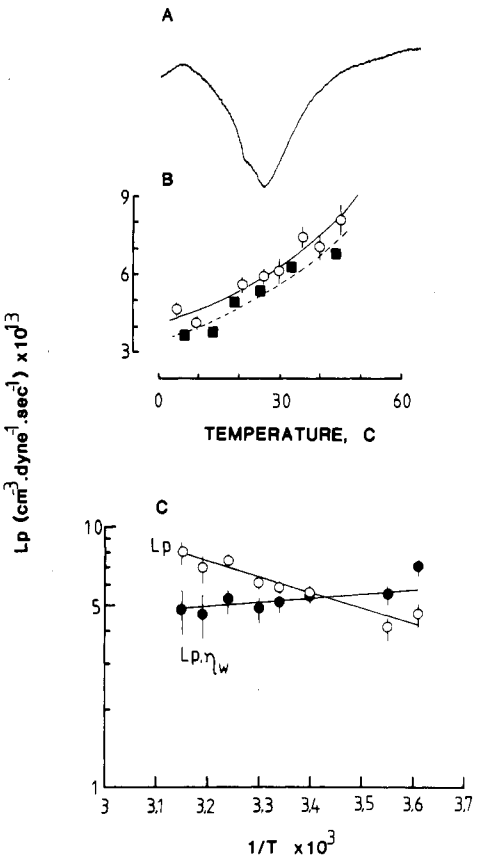

FIGURE 11: Water permeability of protein-enriched LUV bilayers. The bilayers were formed from DPL/egg lecithin [25:75 ratio by weight (○)] and proteins or from egg lecithin (■) and proteins reconstituted at a ratio of 5:100 (protein:lipid) by weight either by detergent dialysis (○) or by reverse-phase evaporation (■). The LUVs contained 20 mM D-glucose and 10 mM KCl. Water flux was measured by injection into 10 mM KCl and 5 μM cytochalasin B. (A) DSC thermogram of 15 μL of packed DPL/egg lecithin LUVs. Scan rate, 10 °C/min. (B) Hydraulic conductivity (Lp) in cubic centimeters per dyne per second of the LUVs vs. temperature; $Lp = P_f/(RT)$ where P_f = the osmotic water permeability coefficient and R and T have their standard meaning. Each point represents the mean (■) or the mean ± SE (○) of at least three measurements. P_f was calculated from dV/dt as described by eq 1. (C) Arrhenius plot of the DPL/egg lecithin data shown in (B) (○). The closed circles represent the Arrhenius plot of the product $Lp\eta w$ where ηw is water viscosity. The straight line through Lp was calculated by the method of least squares and gives an activation energy of 3.2 kcal mol^{-1} K^{-1}. This was used to draw the curve through the points (○) in (B). The line through the points in $Lp\eta w$ was drawn by eye.

Discussion

The high permeability of biological membranes to water has been attributed in part to the rapid flux of water through the lipid phase of the membrane (Conlon & Outhred, 1978). The diffusional exchange of small molecules across protein-free

synthetic membranes depends on the degree of packing and thermal mobility of the hydrocarbon chains and on the charge of the polar head group of the phospholipid (Van Deenen, 1971; Reeves & Dowben, 1970; Papahadjopoulos et al., 1973; Demel et al., 1972). It is not unreasonable, therefore, to expect that the permeability characteristics of biological membranes will be governed to a large extent by these factors. Such a hypothesis, however, ignores the possible influence of membrane proteins on membrane permeability properties. Proteins may facilitate the transbilayer flux of solute or water specifically (e.g., by transport) or nonspecifically, perhaps by forming a low-resistance nonspecific shunt between protein and lipid. Moreover, the various membrane proteins that serve as channels for specific cations may also permit the concomitant transbilayer flux of water. One of our aims was to examine this possibility. Furthermore, we have investigated in detail the effects of altered bilayer physical state and composition on water permeability.

Our methodological approach of measuring turbidity changes of a suspension of vesicles which are undergoing osmotically induced volume changes is based on the assumption that the amount of light scattered by the vesicles is a function of their volume. In theory, the reciprocal of the volume change of spherical particles is not proportional to the first power of the relative light-scattering changes (Koch, 1961). In practice, however, the reciprocal of the volume change is proportional to the change in apparent absorbance when the apparent absorbance is due to light scattering alone. This has been shown experimentally for mitochondria (Tedeschi & Harris, 1955, 1958; Rendi, 1967), erythrocytes (Sidel & Solomon, 1957), microsomes (Kamino & Inouye, 1969), and multilamellar lipid vesicles (Bangham et al., 1967; Bittman & Blau, 1970; Demel et al., 1972; Blok et al., 1976, 1977). We confirm this here for large unilamellar vesicles. A further requirement is that the vesicles behave as perfect osmometers. This requirement is satisfied under the conditions of our experiments and has been reported to be observed with chloroplast grana (Gross & Packer, 1967), microsomes (Kamino & Inouye, 1969), human erythrocytes (Sha'afi et al., 1967), and multilamellar vesicles (Bangham et al., 1967; Bittman & Blau, 1970; Blok et al., 1976). Indeed, liposomes behave as perfect osmometers both above and below their lipid phase transition temperature (Blok et al., 1976). Since the net transmembrane water flux is proportional to the membrane area and the transmembrane osmotic gradient, the large surface area of LUVs permits the measurement, by turbidity change, of the initial rate of volume change, dV/dt, upon rapid change of the osmotic pressure of the suspending medium. Alternative techniques (such as use of ^3H_2O) suffer from a lack of resolution arising from quenching difficulties. Nevertheless, our approach measures the osmotically induced water flow only, and steady-state H_2O exchange rates must be determined by using other methods such as tritiated water or D_2O exchange or NMR (Vieira et al., 1970; Lawaczeck, 1979; Conlon & Outhred, 1978).

A primary determinant of water permeability in protein-free LUVs is bilayer physical state. As the bilayers become more fluid, so permeability increases. Table I shows the magnitude of these permeability changes. The increase in the initial transmembrane water flux on melting the bilayer ranges from 30-fold in DML and DSL LUVs to 130-fold in DPL LUVs. This latter increase arises for the most part from the very low permeability of crystalline DPL bilayers. Following completion of the melt, bilayer water permeability continues to increase with increasing temperature but rather less rapidly than during the melt.

Indeed, water flux in both DEL and egg yolk sphingomyelin LUVs seems to saturate on completion of the liquid-crystalline to fluid phase transition. DOL LUVs also show little increase in water permeability over the temperature range 10–70 °C although the absolute flux is some 17% of that in fluid DEL LUVs. This apparent saturation of water flux with increasing temperature above the phase transition may also be seen with DML, DSL, and DPL. Moreover, our data suggest strongly that the final saturated osmotic permeability coefficient may be the same, within experimental error, for DEL, DSL, DML, and DPL LUVs. It is not immediately obvious why DOL bilayers should be less permeable to water than bilayers formed from the other lecithins. Certainly, the saturated water flux in these latter membranes seems not to be related to chain length or degree of unsaturation of the lipid.

Differential scanning calorimetry of the various lecithin LUVs shows that as in multilamellar lecithin systems the main phase transition of each lipid is preceded by a smaller "pretransition" [see Ranck et al. (1974) and Janiak et al. (1976)]. With multilamellar vesicles, this transition is associated with a structural transformation from a one- to a two-dimensional monoclinic lattice of lipid lamellae with a periodic undulation or ripple. We find no obvious change in water permeability of the lecithin bilayers associated with the pretransition of LUVs.

The water permeability of crystalline lecithin LUVs follows the sequence DEL > DML = DSL > DPL. Again, there is little correlation of chain length or degree of unsaturation of the lipids with water flux. Our results are in agreement with those of Nicolussi et al. (1982) which show that crystalline DML bilayers are more permeable to water than crystalline DPL bilayers. Bittman & Blau (1972) report that at 38 °C, DOL vesicles are some 52-fold more permeable to water than DPL bilayers. We observe a corresponding difference of some 49-fold. Our findings are, therefore, in accord with earlier observations. Papahadjopoulos et al. (1973) noted a complex dependency of $^{22}Na^+$ permeability in DPL and dipalmitoylphosphatidylglycerol vesicles on temperature. A large increase in Na^+ permeability is observed at the midpoint of the phase transition followed by a decrease as temperature is further raised. On completion of the phase transition, permeability increases with temperature. This behavior was not observed here, or in earlier studies (Blok et al., 1976, 1977; Boehler et al., 1978; Lawaczeck, 1979) with water permeability in lecithin LUVs. Blok et al. (1976) have attributed this effect on solute permeability to perturbations in the lipid phase equilibrium resulting from sudden changes in temperature. Here, such temperature changes were avoided by preequilibration of the medium and LUVs at the same temperature.

Experiments with bovine brain and egg yolk sphingomyelin LUVs showed that significant leakage of intravesicular D-glucose occurred when crystalline LUVs were injected into hypotonic medium. This was not apparent from studies with lecithin LUVs, indicating that the viscoelastic properties of crystalline sphingomyelin may differ from those of crystalline lecithin. The binary system of DOL and egg yolk sphingomyelin showed no tendency to lyse at temperatures where much of the sphingomyelin is in the liquid-crystalline state. The depression of the T_m for the sphingomyelin melt in the binary system indicates that some mixing of DOL and sphingomyelin occurred. This may account for the apparent change in the viscoelastic properties of crystalline sphingomyelin in the binary system.

The water permeability characteristics of DML/cholesterol LUVs are complex. In keeping with the findings of Bittman

& Blau (1972), cholesterol reduces water permeability. A number of anomalous effects are apparent, however. At 5 mol % cholesterol and low temperatures, DML LUVs show high permeability, particularly at the midpoint of the phase transition. This effect is lost above this temperature where 5% cholesterol serves to reduce permeability. DSC of the LUVs does not demonstrate any significant event other than the loss of the pretransition. Dilatometry of DPL/cholesterol mixtures, however, illustrates that 5% cholesterol increases the apparent partial specific volume most markedly during the phase transition (Melchior et al., 1980). Moreover, X-ray diffraction studies show that addition of 5 mol % cholesterol to crystalline DML bilayers results in an altered acyl chain configuration from a tilted orientation to an orientation normal to the plane of the bilayer. This effect, which is marked at 23 °C, results in increased spacing between acyl chains (Janiak et al., 1976; Ranck et al., 1974; Hui & He, 1983) and is reflected dramatically in this study as increased water permeability. Between 23 and 35 °C, 5 mol % cholesterol reduces the spacing between the acyl chains (Hui & He, 1983), a finding entirely consistent with our observations. Hui & He (1983) also report (using electron diffraction) a marked increase in the disorder of cholesterol-containing DML bilayers between 37 and 45 mol % cholesterol. This is consistent with the observed increase in water permeability of DML bilayers when the cholesterol content is increased from 34 to 40 and 50 mol %. This disorder is not observed as an increased apparent partial specific volume in cholesterol-containing DPL bilayers (Melchior et al., 1980), but it appears that interactions between DML and cholesterol and DPL and cholesterol may differ somewhat in multilamellar systems (Mabrey et al., 1978). Here, we observe that the osmotic water permeability of DPL LUVs containing 50 mol % cholesterol is only 33% of that of DML LUVs containing 50 mol % cholesterol. Both the heat of the transition and water permeability continue to decrease in DML LUVs with increasing cholesterol content until approximately 27 mol % cholesterol. Thereafter, water permeability increases, and the heat of the transition decreases with increasing cholesterol content. Significant endotherms centering about 22–23 °C are observed at 20–34 mol % cholesterol, indicating that uncomplexed DML is still present in the bilayers. The onset temperature of the broader melt of the presumed DML/cholesterol complex is raised, and the heat of this transition falls with increasing cholesterol content between 20 and 34 mol %. We observe a residual DML melt at both 40 and 50 mol % cholesterol. The heat of these melts is very low. This thermal behavior is not observed in cholesterol-containing DPL multilamellar vesicles and LUVs (Mabrey et al., 1978; Melchior et al., 1980; A. Carruthers and D. L. Melchior, unpublished results).

The water permeability characteristics of binary systems seem to reflect the sum of the characteristics of the lipid constituents. This is well illustrated by DOL and DSL where the water permeability of the binary system is characteristic of DOL bilayers below the DSL melt and increases to an intermediate level above the melt of DSL. The increase in permeability to the intermediate state parallels closely the melt of DSL. With DOL and egg yolk sphingomyelin, the behavior of the binary system is rather more complex, and while permeability reflects, to a large extent, the physical properties of the binary system, there is anomalous behavior at the completion of the sphingomyelin melt. The reasons for this are not obvious, but the behavior persists in DOL/egg yolk sphingomyelin mixtures containing sufficient cholesterol (25 mol %) to abolish the phase transition of sphingomyelin.

Water fluxes in LUVs formed from total lipids extracted from human red blood cells are characteristic of bilayers undergoing a phase transition at about 20–22 °C. Such a transition was not detected by DSC. Nevertheless, a further permeability event in these bilayers beginning at approximately 40 °C correlates well with the presence of a low-heat endotherm (0.3 J/g of lipid) beginning at 36 °C. The low heat of this transition is consistent with the high cholesterol content of these membranes (46 ± 2%). This small endotherm is not observed in packed, white erythrocyte ghosts but may be present in partially cholesterol depleted erythrocyte membranes. Moreover, there is evidence for a further endotherm in partially cholesterol depleted red cell membranes between 0 and 12 °C. These DSC data illustrate that the organization of lipids in the native red cell membrane is quite different from that in bilayers formed in vitro from extracted red cell lipids. This may arise, in part, from the loss of asymmetry in bilayer lipid distribution (Op den Kamp, 1979). Our inability to form LUVs from nominally cholesterol-free red cell lipids may have arisen from the relatively high phosphatidylethanolamine (PE) content (30%) of this mixture. PE forms an unstable bilayer configuration undergoing a bilayer to hexagonal (H_{II}) rearrangement above 0 °C (Taraschi et al., 1982).

The water permeability characteristics of LUVs formed from extracted red cell lipids are rather different from those reported for intact red cells. The permeability coefficient for the self-diffusion of water across the human erythrocyte membrane at 22 °C is 5×10^{-3} cm·s^{-1}. The osmotic permeability coefficient for water is 20×10^{-3} cm·s^{-1} (Vieira et al., 1970; Rich et al., 1968; 40×10^{-3} cm·s^{-1} in this paper). In LUVs formed from extracted red cell lipids, the osmotic water permeability coefficient is on the order of 0.7×10^{-4} cm·s^{-1}. This very low permeability arises in part from the absence of protein. Reconstitution of erythrocyte membrane-spanning proteins into LUVs increases their osmotic water permeability by some 30-fold. This could arise either by flux through water-filled channels (formed by a channel-forming protein) or by flux through the interface between the protein and lipid. This increase in permeability is also observed with D-glucose. With the sugar, the increased permeability is, for the most part, the result of reconstitution of the sugar transport proteins (Jones & Nickson, 1981). Nevertheless, enhanced glucose permeability persists even when protein-mediated transport of D-glucose is abolished by using saturating concentrations of the sugar transport inhibitor cytochalasin B (Widdas, 1980). This enhanced residual glucose permeability of the LUVs may also result from flux via the protein/lipid interface.

The large increase in water permeability on reconstitution of native erythrocyte proteins into synthetic membranes strongly suggests that much of the water permeability of biological membranes is mediated, in some way, by membrane proteins and not by flux via the lipid phase of the membrane. What are the characteristics of this high permeability pathway? If the transbilayer flux of water is mediated via water-filled equivalent pores in the membrane, then hydraulic conductivity, Lp, is described by Poiseuille's law as

$$Lp = nr^4/(8_{\eta w}\Delta X) \qquad (2)$$

where r is the equivalent pore radius, ΔX the path length, ηw the bulk viscosity of water, and n the number of pores per unit area of membrane (Vieira et al., 1970). The only directly temperature-sensitive variable in Lp is ηw. Figure 11 shows that the product $Lp\eta w$ for water flux in DPL/egg lecithin, protein-enriched LUVs is virtually independent of temperature. Essentially identical findings have been described for water flux in the human and dog erythrocyte (Vieira et al., 1970).

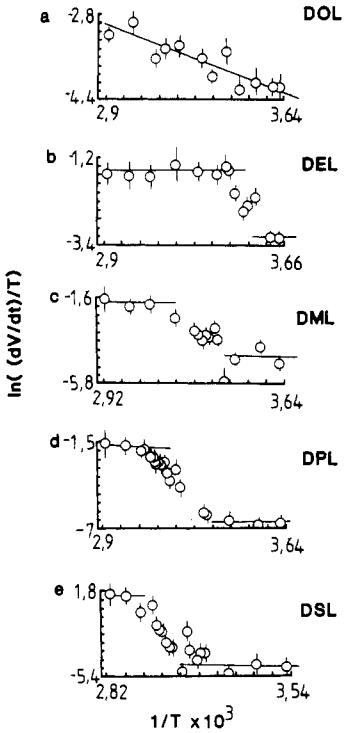

FIGURE 12: Arrhenius plots of the rate of volume change in DOL (a), DEL (b), DML (c), DPL (d), and DSL (e) LUVs. Data points were obtained from Figure 4B. In order to correct for the influence of temperature on the transbilayer osmotic gradient, the points were plotted in the form suggested by Block et al. (1977) as ln $[(dV/dt)/T]$ vs. $1/T$. The lines drawn through the points were obtained by weighted nonlinear regression.

If water permeability in protein-containing bilayers is a protein-mediated phenomenon, how does water traverse protein-free, synthetic bilayers? Two hypotheses have been suggested. Water may permeate by diffusion through transient pores or water-filled channels within the membrane (Pagnelli & Solomon, 1957; Huang & Thompson, 1966; Thompson & Huang, 1966) or by a solubility–diffusion mechanism in which water partitions into the hydrocarbon interior of the bilayer and diffuses through by exchanging between mobile regions of free volume created by thermal fluctuations of the hydrocarbon chains (Träuble, 1971; Lieb & Stein, 1969; Hanai & Haydon, 1966; Finkelstein & Cass, 1968; Reeves & Dowben, 1970; Bittman & Blau, 1972). This problem is not easily resolved. Our data suggest that water permeability is influenced little by the lipid hydrocarbon chain length or the degree of unsaturation. On the other hand, water solubility in hydrocarbons is influenced markedly by chain length and the degree of unsaturation (Schatzberg, 1963; Englin et al., 1965; Reeves & Dowben, 1970). We suggest, therefore, that the solubility–diffusion mechanism cannot account for our observations and that a transient pore mechanism may be more consistent with the data. The number of transient pores may increase with increasing bilayer fluidity, accounting for the marked increase in permeability during the phase transition and the saturation of permeability at higher temperatures. This view is supported to some extent by the complex behaviors of DML/cholesterol bilayers.

Earlier studies (Blok et al., 1976; Boehler et al., 1978; Lawaczeck, 1979) have suggested that water transport across the crystalline bilayer is mediated by a fundamentally different process from that in the fluid bilayer. This hypothesis is based on the demonstration of different activation energies for water flux in fully crystalline and fully fluid bilayers [E_a(crystalline) > E_a(fluid); Blok et al., 1976]. Figure 12 shows that no such difference is apparent in this study. Arrhenius plots of water flux (corrected for the effect of temperature on the osmotic gradient; Blok et al., 1977) show similar slopes above and below the bilayer melt [range of E_a estimates, (2.4 ± 0.6)–(6.5 ± 0.4) kcal mol^{-1} K^{-1}]. The very low activation energies indicate that water flux is virtually independent of temperature. Fluid DOL LUVs show a somewhat greater activation energy for water flux than fluid DEL LUVs. This further emphasizes the differences between DOL bilayers and bilayers formed from the other synthetic lecithins. The similar activation energies for flux in crystalline and fluid membranes are suggestive of a common mechanism for transport where the absolute flux rate is determined solely by the number of transport or permeation sites. The number of these sites may be increased in fluid bilayers.

It is conceivable that water flux is related to the interaction of the lipid polar head groups with water rather than the solubility of water in the lipid hydrocarbon. In any event, the exchange of water between free volume in the hydrocarbon core of the bilayer is kinetically indistinguishable from diffusion through transient pores. This could account for the similar maximum osmotic water permeability coefficients in the various lecithin LUVs and their dependence on the bilayer physical state. Water diffuses–exchanges between the various hydration shells of the polar head group (Hauser & Phillips, 1979) into the hydrocarbon core. The potential energy for this net movement is derived from the transbilayer water concentration (osmotic) gradient. Diffusional flux through the hydrocarbon core is increased with increasing thermal fluctuation of the acyl chains. Divalent cations compete with water for interaction with the negatively charged phospholipid phosphate groups, resulting in the expulsion of water (Hauser et al., 1976). One interesting test of the bound-water exchange–diffusion model might be to determine the effects of various divalent cations on the water permeability characteristics of protein-free synthetic lipid bilayers.

In conclusion, biological membrane water permeability is governed for the most part by the presence of membrane-spanning proteins. Water flux may occur at the lipid/protein interface or via channels formed by proteins. In the absence of protein, water flux is almost 2 orders of magnitude less rapid and is affected markedly by the physical state of the membrane.

Acknowledgments

We thank C. Rodgers and N. Frost for their outstanding work in the design and manufacture of the rapid stop-flow apparatus used in this study. A.C. gratefully acknowledges the award of a Welcome Trust Travel Grant and assistance from the S.E.R.C. of Great Britain and the Muscular Dystrophy Association.

Registry No. Dimyristoyllecithin, 13699-48-4; dipalmitoyllecithin, 2644-64-6; dioleoyllecithin, 10015-85-7; distearoyllecithin, 4539-70-2; dielaidoyllecithin, 52088-89-8; cholesterol, 57-88-5; water, 7732-18-5; D-glucose, 50-99-7.

References

Ackman, R. G. (1981) *Methods Enzymol. 72*, 205–252.
Avramovic-Zikic, O., & Colbow, K. (1978) *Biochim. Biophys. Acta 512*, 97–104.
Bangham, A. D., Standish, M. M., & Watkins, J. C. (1965) *J. Mol. Biol. 13*, 238–245.
Bangham, A. D., de Gier, J., & Greville, G. D. (1967) *Chem. Phys. Lipids 1*, 225–246.
Bartlett, G. R. (1959) *J. Biol. Chem. 234*, 466–468.
Bittman, R., & Blau, L. (1972) *Biochemistry 11*, 4831–4839.

Bligh, E. G., & Dyer, W. J. (1959) *Can. J. Biochem. 37*, 911–918.
Blok, M. C., van Deenen, L. L. M., & de Gier, J. (1976) *Biochim. Biophys. Acta 433*, 1–12.
Blok, M. C., van Deenen, L. L. M., & de Gier, J. (1977) *Biochim. Biophys. Acta 464*, 509–518.
Boehler, B. A., de Gier, J., & van Deenen, L. L. M. (1978) *Biochim. Biophys. Acta 512*, 480–488.
Carruthers, A., & Melchior, D. L. (1983) *Biochim. Biophys. Acta 728*, 254–266.
Chong, C. S., & Colbow, K. (1976) *Biochim. Biophys. Acta 436*, 260–282.
Conlon, T., & Outhred, R. (1978) *Biochim. Biophys. Acta 511*, 408–418.
De Gier, J., Haesk, C. W. M., Mandersloot, J. G., & van Deenen, L. L. M. (1970) *Biochim. Biophys. Acta 211*, 373–375.
Demel, R. A., Bruckdorfer, K. R., & van Deenen, L. L. M. (1972) *Biochim. Biophys. Acta 255*, 321–330.
Englin, B. A., Plate, A. F., Tugolukov, V. M., & Pryanishnikov, M. A. (1965) *Khim. Tekhnol. Topl. Masel 10*, 42–57.
Finklestein, A., & Cass, A. (1968) *J. Gen. Physiol. 52*, 145S–173S.
Gamble, W., Vaughan, M., Kruth, H. S., & Avigan, J. (1978) *J. Lipid Res. 19*, 1068–1070.
Gross, E. L., & Packer, L. (1967) *Arch. Biochem. Biophys. 121*, 779–798.
Hanai, T., & Haydon, D. A. (1966) *J. Theor. Biol. 11*, 370–382.
Hauser, H., & Phillips, M. C. (1979) *Prog. Surf. Membr. Sci. 13*, 297–413.
Hauser, H., Darke, A., & Phillips, M. C. (1976) *Eur. J. Biochem. 62*, 335–344.
Huang, C., & Thompson, T. E. (1966) *J. Mol. Biol. 15*, 539–554.
Hui, S. W., & He, N.-B. (1983) *Biochemistry 22*, 1159–1164.
Janiak, M. J., Small, D. M., & Shipley, G. G. (1976) *Biochemistry 15*, 4575–4580.
Jones, M. N., & Nickson, J. K. (1981) *Biochim. Biophys. Acta 650*, 1–20.
Kamino, K., & Inouye, A. (1969) *Biochim. Biophys. Acta 183*, 36–47.
Kasahara, M., & Hinkle, P. C. (1977) *J. Biol. Chem. 252*, 7384–7390.
Koch, A. L. (1961) *Biochim. Biophys. Acta 51*, 429–441.
Lawaczeck, R. (1979) *J. Membr. Biol. 51*, 229–261.
Lieb, W. R., & Stein, W. D. (1969) *Nature (London) 224*, 240–243.
Lowry, O. H., Rosebrough, N. J., Farr, A. L., & Randall, R. J. (1951) *J. Biol. Chem. 193*, 265–275.
Mabrey, S., Mateo, P. L., & Sturtevant, J. M. (1978) *Biochemistry 17*, 2464–2468.
Masaik, S. J., & LeFevre, P. G. (1974) *Arch. Biochem. Biophys. 162*, 442–447.
Melchior, D. L., Scavitto, F. J., Walsh, M. T., & Steim, J. M. (1977) *Thermochim. Acta 18*, 43–71.
Melchior, D. L., Scavitto, F. J., & Steim, J. M. (1980) *Biochemistry 19*, 4828–4834.
Nicolussi, A., Massari, S., & Colonna, R. (1982) *Biochemistry 21*, 2134–2140.
Op den Kamp, J. A. F. (1979) *Annu. Rev. Biochem. 48*, 47–71.
Pagnelli, C. V., & Solomon, A. K. (1957) *J. Gen. Physiol. 41*, 259–278.
Papahadjopoulos, D., Jacobson, K., Nir, S., & Isac, T. (1973) *Biochim. Biophys. Acta 311*, 330–348.
Ranck, J. L., Mateu, L., Sadler, D. M., Tardieu, A., Gulik-Krzywicki, T., & Luzzati, V. (1974) *J. Mol. Biol. 85*, 249–277.
Reeves, J. P., & Dowben, R. M. (1970) *J. Membr. Biol. 3*, 123–141.
Rendi, R. (1967) *Biochim. Biophys. Acta 135*, 333–346.
Rich, G. T., Sha'afi, R. I., Romualdez, A., & Solomon, A. K. (1968) *J. Gen. Physiol. 52*, 941–954.
Schatzberg, P. (1963) *J. Phys. Chem. 67*, 776–779.
Sha'afi, R. I., Rich, G. T., Sidel, V. W., Bossert, W., & Solomon, A. K. (1967) *J. Gen. Physiol. 50*, 1377–1399.
Sidel, V. W., & Solomon, A. K. (1957) *J. Gen. Physiol. 41*, 243–261.
Szoka, F., Jr., & Papahadjopoulos, D. (1980) *Annu. Rev. Biophys. Bioeng. 9*, 467–508.
Takemoto, Y. (1980) *Kawasaki Med. J. 6*, 1–18.
Taraschi, T. F., de Kruijff, B., Verkleij, A., & van Echteld, C. J. A. (1982) *Biochim. Biophys. Acta 685*, 153–161.
Tedeschi, H., & Harris, D. L. (1955) *Arch. Biochem. Biophys. 58*, 52–63.
Tedeschi, H., & Harris, D. L. (1958) *Biochim. Biophys. Acta 28*, 392–401.
Thompson, T. E., & Huang, C. (1966) *Ann. N.Y. Acad. Sci. 137*, 740–744.
Träuble, H. (1971) *J. Membr. Biol. 4*, 193–208.
van Deenen, L. L. M. (1971) *Pure Appl. Chem. 25*, 25–57.
Vieira, F. L., Sha'afi, R. I., & Solomon, A. K. (1970) *J. Gen. Physiol. 55*, 451–466.
Weissman, G., Sessa, G., & Weissman, S. (1966) *Biochem. Pharmacol. 15*, 1537–1541.
Widdas, W. F. (1980) *Curr. Top. Membr. Transp. 14*, 165–223.
Yi, P. N., & Mac Donald, R. C. (1973) *Chem. Phys. Lipids 11*, 114–134.